PLOS ONE

RESEARCH ARTICLE

Identification, expression and functional characterization of M_4L, a muscarinic acetylcholine M_4 receptor splice variant

Douglas A. Schober[1], Carrie H. Croy[1], Cara L. Ruble[1], Ran Tao[2], Christian C. Felder[1]*

1 Neuroscience, Lilly Research Laboratories, Lilly Corporate Center, Eli Lilly and Company, Indianapolis, Indiana, United States of America, **2** Lieber Institute for Brain Development, Baltimore, Maryland, United States of America

* felder_christian@lilly.com

Citation: Schober DA, Croy CH, Ruble CL, Tao R, Felder CC (2017) Identification, expression and functional characterization of M_4L, a muscarinic acetylcholine M_4 receptor splice variant. PLoS ONE 12(12): e0188330. https://doi.org/10.1371/journal.pone.0188330

Editor: Emanuele Buratti, International Centre for Genetic Engineering and Biotechnology, ITALY

Received: August 9, 2017

Accepted: November 3, 2017

Published: December 6, 2017

Data Availability Statement: All relevant data are within the paper.

Funding: Funding for this study was supported by Eli Lilly and Company, a commercial organization and the Lieber Institute for Brain Development, a non-profit Maryland Medical Research Institution affiliated with The Johns Hopkins University School of Medicine. The Eli Lilly and Company and LIBD provided support in the form of salaries for authors DAS, CCF, CHC, CLR and RT, respectively. They did not have any additional role in the study design,

Abstract

Rodent genomic alignment sequences support a 2-exon model for muscarinic M4 receptor. Using this model a novel N-terminal extension was discovered in the human muscarinic acetylcholine M_4 receptor. An open reading frame was discovered in the human, mouse and rat with a common ATG (methionine start codon) that extended the N-terminus of the muscarinic acetylcholine M_4 receptor subtype by 155 amino acids resulting in a longer variant. Transcriptional evidence for this splice variant was confirmed by RNA-Seq and RT-PCR experiments performed from human donor brain prefrontal cortices. We detected a human upstream exon indicating the translation of the mature longer M_4 receptor transcript. The predicted size for the longer two-exon M_4 receptor splice variant with the additional 155 amino acid N-terminal extension, designated M_4L is 69.7 kDa compared to the 53 kDa canonical single exon M_4 receptor (M_4S). Western blot analysis from a mammalian overexpression system, and saturation radioligand binding with [^{3}H]-NMS (N-methyl-scopolamine) demonstrated the expression of this new splice variant. Comparative pharmacological characterization between the M_4L and M_4S receptors revealed that both the orthosteric and allosteric binding sites for both receptors were very similar despite the addition of an N-terminal extension.

Introduction

The endogenous neurotransmitter, acetylcholine, binds to both nicotine-sensitive ion channels and muscarinic-sensitive GPCRs (G-protein coupled receptors). The muscarinic family contains 5 known Class A, membrane protein receptor subtypes (M_1-M_5) that originate from distinct genes. The M_4 receptor is highly expressed in the striatum, cortex, and hippocampus, areas involved in mood, cognition, and drug seeking behaviors. However, relatively little is known about the physiological function of the M_4 receptor as selective pharmacological tools have only recently been developed [1]. Selective M_4 positive allosteric modulators have shown efficacy similar to both typical and atypical antipsychotics in animal models predictive of

data collection and analysis, decision to publish, or preparation of the manuscript. The specific roles of these authors are articulated in the 'author contributions' section.

Competing interests: This study received funded in the form of salaries from Eli Lilly and Company and the Lieber Institute for Brain Development. There are no patents, products in development or marketed products to declare. This does not alter the authors' adherence to all the PLOS ONE policies on sharing data and materials, as detailed online in the guide for authors.

schizophrenia [2, 3]. The M_4 receptor plays an inhibitory role on presynaptic terminals and regulates neurotransmitter release in both an autoreceptor role (acetylcholine) and hetero-receptor role (e.g. dopamine, GABA, serotonin) depending on brain region localization [4]. To date no mouse, rat or human splice variants of the muscarinic receptors that generate novel proteins have been characterized.

Many GPCRs were thought to originate from single exon genes. The recognition of introns within the coding regions of GPCRs has increased gradually from 10% [5] to 52% [6]. Subject to conditional, temporal, and cell-type regulation, alternative splicing can generate structurally similar proteins with functionally identical or significantly different properties [7] effecting signaling and/or pharmacology [8]. Alternatively spliced GPCR isoforms can differ in their abilities to undergo post-translational modification and/or to interact with accessory proteins which also can greatly influence their biological activity [6].

The extracellular N-terminal extension of M_4 is short (31 amino acids) compared to other neurotransmitter receptors which typically have long N-terminal segments [9]. The curated transcript sequence in GenBank (NM_00741) transcribes a 1.8 kb product, and the protein sequences (NP_000732) translates into a 53 kDa protein. However published work such as Buchli et al which show experimental northern blot data estimating an M_4 receptor transcript size of 4.8 kb and a Western blot reactive-protein estimated at 70 kDa [10]. These size discrepancies led us to explore the M_4 receptor for transcriptional diversity. Expressed Sequence Tags (ESTs) analyses were used to identify additional exons, and comparative genomics analyses were used to identify putative 5'extensions of the open reading frame (ORF). These analyses when performed on rodent and human genomic databases revealed an alternative M_4 receptor transcript that would increase the extracellular N-terminus by 155 amino acids. Human neuronal RNA-seq data was then interrogated and confirmed the existence of the splice junctions, and the mature mRNA was experimentally confirmed by RT-PCR. Further experiments were performed to confirm and characterize the longer M_4-receptor variant (M_4L) protein. Overall the binding and functional pharmacology studies characterized and compared the human muscarinic M_4L receptor splice variant that encodes an additional 155 amino acids on the N-terminus to that of the canonical single exon M_4 receptor protein in an overexpressed cellular model.

Materials and methods

Human tissues, RNA extraction and quality assessment, RNA-seq library construction, RNA sequence mapping

Human tissues samples used in this study were part of an early-stage research consortium BrainSEQ™ with the Lieber Institute of Brain Development (LIBD), with the goal of expanding knowledge around the genetic contribution to brain disorders. The LIBD postmortem human brain collection contains samples acquired through an informed consent from relatives of the deceased for 751 postmortem human brain samples through the Office of the Chief Medical Examiner of the State of Maryland. Additionally, the collection has 1,213 postmortem human brain tissue samples acquired via material transfer agreements, including those from the National Institute of Mental Health (NIMH), the Eunice Kennedy Shriver National Institute of Child Health and Development (NICHD) Brain Bank, the Stanley Medical Research Institute, and The Johns Hopkins University. All brain donations were obtained by verbal, witnessed informed consent with the next-of-kin (protocol #90-M-0142 approved by the NIMH/NIH Institutional Review Board). RNA-Seq datasets from the dorsal lateral prefrontal cortex (DL-PFC) of 211 donors contained an average of 114 million reads per sample, with an average of 81% mapping rate to the reference genome were previously described in Ruble *et al* [11].

Genomic DNA comparisons were done with ACT: the Artemis Comparison Tool [12]. Sim4 was used for aligning mRNA and EST sequences [13]. Open Reading Frame analysis was done using Sequencher® version 5.1 sequence analysis software, Gene Codes Corporation, Ann Arbor, MI USA http://www.genecodes.com. The EMBOSS suite was used for sequence extraction and calculation of molecular weights [14]. Multiple alignments were created using MUSCLE [15] and viewed using GeneDoc [16]. RNA-seq reads were aligned to the human genome reference with GSNAP [17] and visualized using OmicSoft® ArrayStudio® software, version 10.

PCR and sequence confirmation

To verify the splicing variants of M_4 in human brain, we performed exon-to-exon PCR using 3 brain total RNA with M_4 gene specific sense primers binding at exon 1 using SMART RACE cDNA Amplification Kit (Clonetech) and Advantage 2 PCR Kit (Clonetech). The human brain total RNA was reverse-transcribed to cDNA by MMLV reverse transcriptase (Clontech) according to the manufacturer's protocol. Based on RNA sequencing, we designed primer pairs to verify the M_4 splice variants using Platinum TaqDNA polymerase (Invitrogen). The control primer set to detect the canonical M_4 transcript was `TCCCACA ATCGCTATGAGACG` (forward) and `CACCACAAACTGCCAGAACAAG` (reverse). Junction primers were designed to bridge between the short and long transcripts (`GTCCGTCCCGC CGTCTGTCT` (forward) and `CGTTGCTCACCACGTAGTCC` (reverse)). The PCR conditions were 94˚C for 3 min, 35 cycles of 94˚C for 30 sec, 60˚C for 30 sec, 72˚C for 1 min, and 72˚C for 10 min after the last cycle. The PCR products were cloned into E. coli by PCR-TOPO 4.0 vectors (InvitrogenTM) and sequenced [18]. All PCR results were confirmed in separate PCR assays and Sanger sequencing.

Western blot assays

Protein was extracted from cell pellets using RIPA buffer and protease inhibitors and soluble protein lysate from this preparation was quantified using Coomassie Plus Protein Assay (Thermo-Fisher). Lysates were normalized by total protein and 10μg loaded on a 4–20% Tris-Glycine gradient gel (Novex, Life Technologies). Samples were transferred onto PVDF membranes, membranes were blocked with 5% nonfat milk phosphate-buffered saline with 0.1% Tween-20 (PBS-T) (Sigma-Aldrich, P9416) for 1h at room temperature prior to antibody incubation. The muscarinic M_4 receptor was N-terminal tagged with c-MYC so that we could use a rabbit primary antibody which recognized myc epitope (Millipore, 05–724, 1:1000 in 5% milk PBS-T) In addition, a beta actin loading control mouse monoclonal antibody (ThermoFisher, MA5-15739, 1:1000 in 5% milk PBS-T was used to normalize the Western blot. Both antibodies were incubated overnight at 4˚C. Blots were washed in PBS-T then probed with mouse and rabbit IRDye secondary antibodies (Li-COR, 1:15,000, 5% milk. PBS-T) and visualized by the Li-COR Odyssey® Imaging system.

Immunofluorescence

Immunofluorescence analysis of HEK293T (ATCC, CRL-3216) transiently expressing M_4 receptor were carried out by labelling the constructs N-terminal myc-epitope. Specifically, cells were fixed with 4% paraformaldehyde, permeabilized with 0.25% Triton X-100, blocked in 5% normal goat-serum, incubated with anti-myc 1:1000 (anti-myc, clone A46, Millipore 05–724), and detected via the Alexa Fluor 488-conjugated goat anti-mouse IgG (1:500, Jackson Immunologics) secondary antibody. Hoerst stain (blue) was used as the nuclear counterstain.

[^{3}H]-NMS binding assays

[^{3}H]-NMS (PerkinElmer, NET636001MC) saturation binding assays were performed in HEPES buffer [20mM HEPES (Sigma-Aldrich, H0887), 100mM NaCl (S5150), 10mM $MgCl_2$ (M1028), pH 7.4]. Equilibrium binding was achieved by incubating 3–5μg of muscarinic-containing membranes (human M_4S or M_4L transiently expressed in HEK293T cells) and various concentrations of [^{3}H]-NMS (0.01-2nM) for 2h at 25˚C. Bound [^{3}H]-NMS (fmol/mg membrane) vs. NMS concentration (nM) was fit to a one-site specific binding model using Prism 6.7 (GraphPad Software, Inc.) and was used to calculate B_{max} and K_d values. [^{3}H]-NMS (~0.35nM) displacement assays were performed for 2h at 25˚C in HEPES buffer with membranes (5–10μg) containing either M_4S or M_4L in the presence of varying concentrations (0.1-10mM) of a M_4-PAM (positive allosteric modulator), LY2033298 (Lilly) and acetylcholine (Ach) (Sigma-Aldrich, A6625. All reactions were stopped by rapid filtration on a TOMTEC 96-well cell harvester. Non-specific binding was determined using atropine (10μM) (Sigma-Aldrich, A0132) for both the saturation and displacement binding assays. Radioactivity retained on the filter-mat was counted on a Wallac 1205 Beta-plate scintillation spectrophotometry. The specific binding vs. concentration fit to a one-site K_i model using GraphPad Prism 6.7 using established [^{3}H]-NMS K_d values.

GTP-γ-[^{35}S] binding assays

The level of G protein activation was measured by the amount of non-hydrolyzable GTP-γ-[^{35}S] bound to Gαi- subunit. The GTP-γ-[^{35}S] (PerkinElmer, NEG030X001MC) binding was determined using a WGA SPA-bead technique. GTP-γ-[^{35}S] binding was produced by incubating 50μg of membranes expressing the human M_4S or M_4L variants in assay buffer (20mM HEPES, 100mM NaCl, 0.2μM EDTA, 1μM GDP and 10mM $MgCl_2$, pH 7.4), 500pM GTP- γ -[^{35}S], and varying concentrations of orthosteric muscarinic agonists (acetylcholine, oxotremorine-M and McN-A-343 and pilocarpine). Binding proceeded for 45 min at room temperature with mixing. The Gα-subunits were then captured during a 3h room temperature incubation using a WGA-conjugated SPA beads (Perkin Elmer, 1 mg/reaction). The radioactivity counts of the bound GTP-γ-[^{35}S] were determined by scintillation spectrophotometry (Wallac TriLux, Perkin Elmer). An EC_{50} value was determined by fitting the agonist response using a three-parameter fit model (GraphPad Prism 6.7)

Results and discussion

In silico comparative genomics of the M_4 splice variant

A model of the predicted amino acid sequence for the M_4L splice variant described in this manuscript can be found illustrated in Fig 1.

BY250825.1 and CJ145250.1 are mouse ESTs that have two exons. DV213670.1 is a rat EST that also has two exons. These three ESTs were still "open" on the 5' end relative to the open reading frame (ORF). The splice sites identified in the mouse and rat genomes for these three ESTs are conserved in the human genome. Comparative genomics suggests that an extension of the ORF is possible in human, mouse and rat up to a common ATG/methionine that could possibly extend the amino terminus by 155aa (from 31aa to 186aa for an amino terminus). The extended ORF of the three species is shown as an alignment in Fig 2.

The new Kozak consensus would be GtC cCC ATG and the new mRNA size (2 exons: new ATG to donor, acceptor to polyA signal) would be 3225 bp, and the new protein size would be 69.7 kDa.

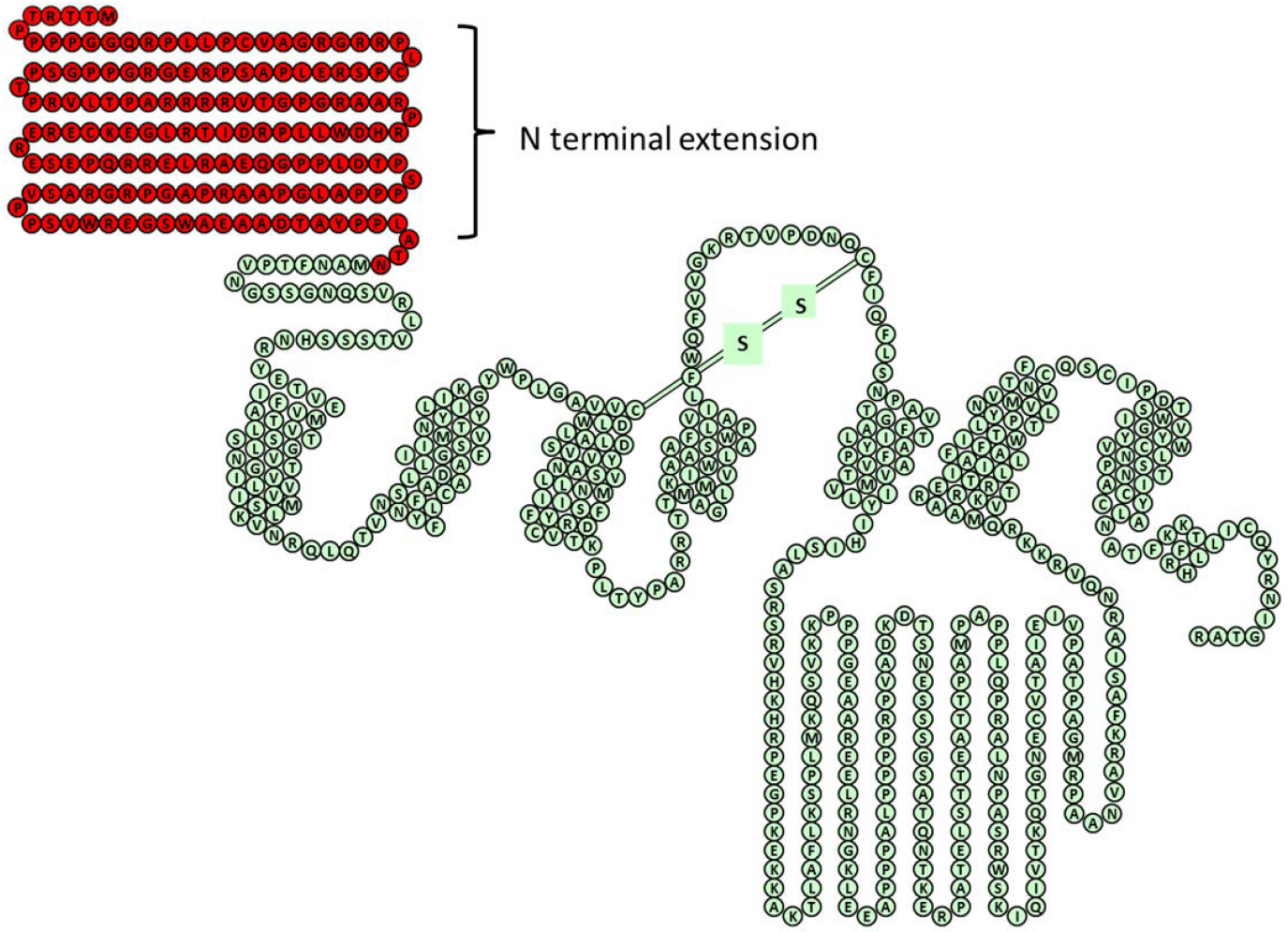

Fig 1. An amino acid sequence model of the muscarinic acetylcholine M_4 receptor. Green represents the canonical sequence of the M_4 receptor while red depicts the 155aa N-terminal extension.

https://doi.org/10.1371/journal.pone.0188330.g001

RNA-seq evidence for the existence of an M_4 splice variant

The 211 human dorsolateral prefrontal cortex (DL-PFC) dataset confirmed the human splice junction of interest (11:46408136-^-46413169) that was originally identified from the rodent ESTs (Fig 3).

The upstream exon to create M_4L was identified in 192 samples with 1426 total junction reads. Junctions Per Million reads Mapped (JPM) was calculated for each sample: JPM = (Junction Count) * 1000000 / (Total Reads Mapped). The average JPM is 0.08 and ranged from 0.86 to 0.

PCR experimentation and sequence confirmation

Using the M_4L transcript as our template (Fig 4), the following PCR primers were designed: The control primer set used to detect the canonical M_4 transcript are highlighted in yellow while the junction primers designed to bridge between the short and long transcripts are highlighted in blue. Reverse transcription polymerase chain reaction (RT-PCR) reactions were performed on 3 human donor samples and their PCR products illustrated in Fig 4.

```
                *         20          *         40          *         60          *         80
human  :  ATGACAACGCGGACA------CCCCCACCCCCCGGAGGGCAGCGCCCCCTGCTCCCCTGCGTCGCTGGCCGTGGGCGGCGCCCTCTGTG  :  83
mouse  :  ATGACAACGCGGACAGCCCCCACCCCACCCCCCGGAGGGCAGAGCCGGAGGCTAATCCTCCCTGGCGACTGTGGGCGGTGCCCTCGGTG  :  89
rat    :  ATGACAACGCGGACAGCCCCCACCCCACCCCCCGGAGGGCAGCGCCGGAGGCTAATCCTCCCTGGCGACTGTGGGCGGTGCCCTCGGAG  :  89

          *       100         *       120         *       140         *       160         *       1
human  :  CCCAAGCAGGGAGCTGCCGGCCAGCCCCCGAGAGGGGCGCGGACCGCCGGGGTCTCCGACGCCTCGGGTGTTGACCCCCGCGCGTCGCC  :  172
mouse  :  CTGGAGTCCGGAGTTGCGGGCCATCTCCCGGGAAGGGTGTGAGCATCAAGGGTGCCTGACACTCCAGGTGGTGACCCCCGCGCGTCGCC  :  178
rat    :  CTGGAGTCCCGAGGCGCGGGCCATCTCTCGGGAAGGGTGTAAGCATCAAGGGTGCCCTACACTCCAGGTGGTGACCCCCGCGCGTCGCC  :  178

          80          *       200         *       220         *       240         *       260
human  :  GCCGGGTGACCGGCCCGGGGCGGGCGGCGCGGCCCCGCCACGATTGGCTGCTTCCTCGTGACATCACGCGGCTCGGGGAAAAGTGCGAG  :  261
mouse  :  GCTGGGTGACCGGCCCCGGGCGGGCGGTGCGTCCCCACCACGATTGGCTGCTTCCCTGTGACATCACGCGGCTCGGAGAAAAGTGCGAG  :  267
rat    :  GCTGGGTGACCGGCCCCGGGCGGGCGGTGCGTCCCCACCACGATTGGCTGCTTCCCTGTGACATCACGCGGCTCGGGGAAAAGTGCGAG  :  267

            *       280         *       300         *       320         *       340         *
human  :  CGTGAGCGCGAGTCGGAGCCACAGCGCCGGGAGCTGCGGGCGGAGCAGGGGCCGCCCCTCGACACCCCGTCCCCGCCCCCGGCCCTCGG  :  350
mouse  :  CGTGAGCGCGAGTCGGAGCCACAGCGCCGGGAGCTGCAGGCGAAGCAGGGGCCGCCCCTTGGCACCCTGTCCCCGCCCCCGGCCCCCGG  :  356
rat    :  CGTGAGCGCGAGTCGGAGCCACAGCGCCCGGAGCTGCAGGCGAAGCAGGGGCCGCCCCTTGGCACCCTGTCCCCGCCCCCGGCCCCCGG  :  356

           360         *       380         *       400         *       420         *       440
human  :  CCCGGCCGCCCGCCCCGCCGGCCCGCGGGGCCGCGCGTCCGTCCCGCCGTCTGTCTGGCGCGAGGGGAGCTGGGCAGAGGCGGCGG  :  436
mouse  :  CCCAGTCGCCCACCCCACCGACTCGCAGGGCCTCTGGCTAGTTCCGCCGTCTGTCCGGCGCCAGCGGAGCAAGACAGAAGCAGCGG  :  442
rat    :  CCCAGTCGCCCACCCCACCGACTCGCGGAACCTCTGGCTTGTTCCGCCGTCTGTCCGGCACCAGCAGAGAAAGACAGAAGCAGCGG  :  442
```

Fig 2. Upstream exon sequence alignments between human, mouse and rat. The underlined nucleotides in mouse and rat correspond to the EST sequences of BY250825.1, CJ145250.1, and DV213670.1.

https://doi.org/10.1371/journal.pone.0188330.g002

Using splice junction-specific primers, RT-PCR experiments were performed to detect the junctions between the canonical M_4 exon and the putative upstream exon within mature mRNAs from 3 different donor brains samples. Using the M_4L transcript, the control primer set (shown in yellow) were used to detect the canonical M_4 transcript while the junction primers designed to bridge between the short and long transcripts are highlighted in blue. The canonical start codon (ATG) is shown in red. RT-PCR reactions were performed on 3 human donor samples and their PCR products. All three samples were DL-PFC from control Caucasian female donors. Sample 1 (lanes 1&2) was from a 75 year old with a 50h PMI (postmortem interval), sample 2 (lanes 3&4) from an 83 year old with a 33.5h PMI and sample 3 (lanes 5&6) from a 49 year with a 36h PMI. Blue andyellow boxes represent the primer pairs mentioned above. All three samples were DL-PFC from control Caucasian female donors. Sample 1 (lanes 1&2) was from a 75 year old with a 50h PMI, sample 2 (lanes 3&4) from an 83 year old with a

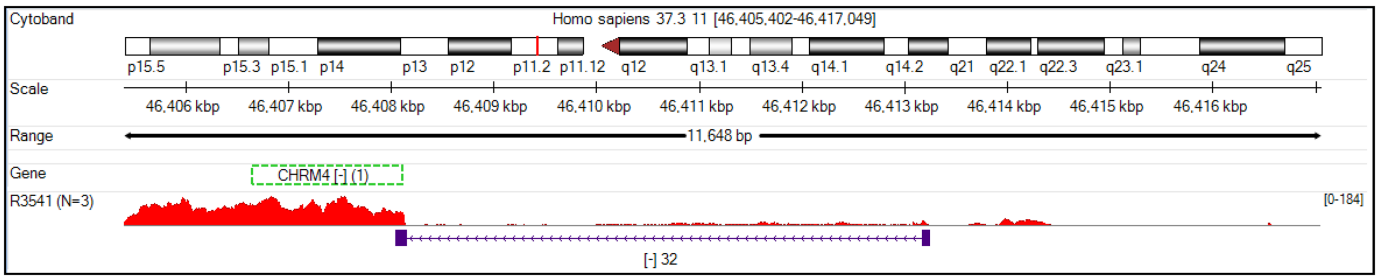

Fig 3. Junction reads through the M_4L transcript from a human prefrontal cortex sample using OmicSoft Array suite.

https://doi.org/10.1371/journal.pone.0188330.g003

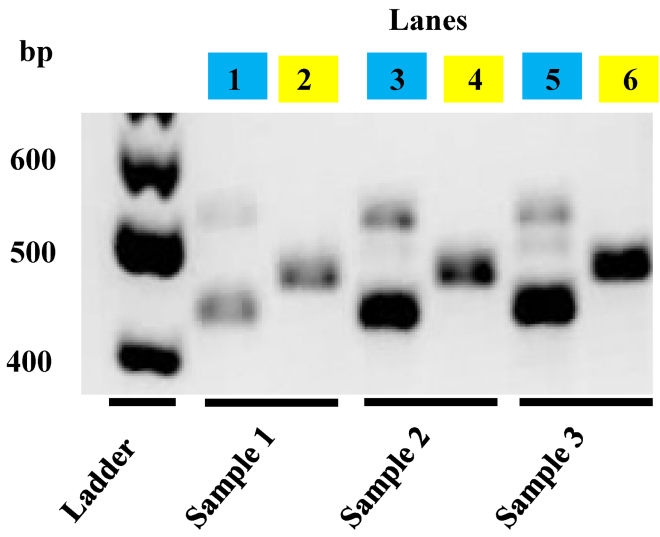


```
ATGACAACGCGGACACCCCCACCCCCCGGAGGGCAGCGCCCCCTGCTCCCCTGCGTCGCTGGCCGTGGGCGGCGCCCTCT :   80
GTGCCCAAGCAGGGAGCTGCCGGCCAGCCCCCGAGAGGGGCGCGGACCGCCGGGGTCTCCGACGCCTCGGGTGTTGACCC : 160
CCGCGCGTCGCCGCCGGGTGACCGGCCCGGGGCGGGCGGCGCGGCCCCGCCACGATTGGCTGCTTCCTCGTGACATCACG : 240
CGGCTCGGGGAAAAGTGCGAGCGTGAGCGCGAGTCGGAGCCACAGCGCCGGGAGCTGCGGGCGGAGCAGGGGCCGCCCCT : 320
CGACACCCCGTCCCCGCCCCCGGCCCTCGGCCCGGCCGCCCGCCCCGCCGGCCCGCGGGGCCGCGCGTCCGTCCCGCCGT : 400
CTGTCTGGCGCGAGGGGAGCTGGGCAGAGGCGGCGGACACGGCCTACCCACCCCTGGCAACCAACATGGCCAACTTCACA : 480
CCTGTCAATGGCAGCTCGGGCAATCAGTCCGTGCGCCTGGTCACGTCATCATCCCACAATCGCTATGAGACGGTGGAAAT : 560
GGTCTTCATTGCCACAGTGACAGGCTCCCTGAGCCTGGTGACTGTCGTGGGCAACATCCTGGTGATGCTGTCCATCAAGG : 640
TCAACAGGCAGCTGCAGACAGTCAACAACTACTTCCTCTTCAGCCTGGCGTGTGCTGATCTCATCATAGGCGCCTTCTCC : 720
ATGAACCTCTACACCGTGTACATCATCAAGGGCTACTGGCCCCTGGGCGCCGTGGTCTGCGACCTGTGGCTGGCCCTGGA : 800
CTACGTGGTGAGCAACGCCTCCGTCATGAACCTTCTCATCATCAGCTTTGACCGCTACTTCTGCGTCACCAAGCCTCTCA : 880
CCTACCCTGCCCGGCGCACCACCAAGATGGCAGGCCTCATGATTGCTGCTGCCTGGGTACTGTCCTTCGTGCTCTGGGCG : 960
CCTGCCATCTTGTTCTGGCAGTTTGTGGTGGGTAAGCGGACGGTGCCCGACAACCAGTGCTTCATCCAGTTCCTGTCCAA : 1040
CCCAGCAGTGACCTTTGGCACAGCCATTGCTGCCTTCTACCTGCCTGTGGTCATCATGACGGTGCTGTACATCCACATCT : 1120
CCCTGGCCAGTCGCAGCCGAGTCCACAAGCACCGGCCCGAGGGCCCGAAGGAGAAGAAAGCCAAGACGCTGGCCTTCCTC : 1200
AAGAGCCCACTAATGAAGCAGAGCGTCAAGAAGCCCCCGCCCGGGGAGGCCGCCCGGGAGGAGCTGCGCAATGGCAAGCT : 1280
GGAGGAGGCCCCCCCGCCAGCGCTGCCACCGCCACCGCGCCCCGTGGCTGATAAGGACACTTCCAATGAGTCCAGCTCAG : 1360
GCAGTGCCACCCAGAACACCAAGGAACGCCCAGCCACAGAGCTGTCCACCACAGAGGCCACCACGCCCGCCATGCCCGCC : 1440
CCTCCCCTGCAGCCGCGGGCCCTCAACCCAGCCTCCAGATGGTCCAAGATCCAGATTGTGACGAAGCAGACAGGCAATGA : 1520
GTGTGTGACAGCCATTGAGATTGTGCCTGCCACGCCGGCTGGCATGCGCCCTGCGGCCAACGTGGCCCGCAAGTTCGCCA : 1600
GCATCGCTCGCAACCAGGTGCGCAAGAAGCGGCAGATGGCGGCCCGGGAGCGCAAAGTGACACGAACGATCTTTGCCATT : 1680
CTGCTAGCCTTCATCCTCACCTGGACGCCCTACAACGTCATGGTCCTGGTGAACACCTTCTGCCAGAGCTGCATCCCTGA : 1760
CACGGTGTGGTCCATTGGCTACTGGCTCTGCTACGTCAACAGCACCATCAACCCTGCCTGCTATGCTCTGTGCAACGCCA : 1840
CCTTTAAAAAGACCTTCCGGCACCTGCTGCTGTGCCAGTATCGGAACATCGGCACTGCCAGGTAG : 1905
```

Fig 4. RT-PCR primer design and results.

https://doi.org/10.1371/journal.pone.0188330.g004

33.5h PMI and sample 3 (lanes 5&6) from a 49 year with a 36h PMI. Using the control primer set (yellow) to detect the canonical M_4 transcript in each of these samples, their PCR product can be seen in lanes 2, 4 and 6. The expected size of this primer combination was a 459bp product. The combination of the junction primers (blue) in lanes 1, 3 and 5 were designed to detect the junction of the canonical M_4 exon with the putative upstream exon within a mature mRNA. The expected size of this primer combination was a 431bp product. Finally, the PCR products were cut and sequenced to confirm the existence of the junction for M_4L. Fig 5 shows that the three human donor samples contain the putative upstream exon sequence; the sequences were aligned with the upstream M_4L exon sequence (top sequence) and the canonical M_4S exon 1 sequence (bottom).

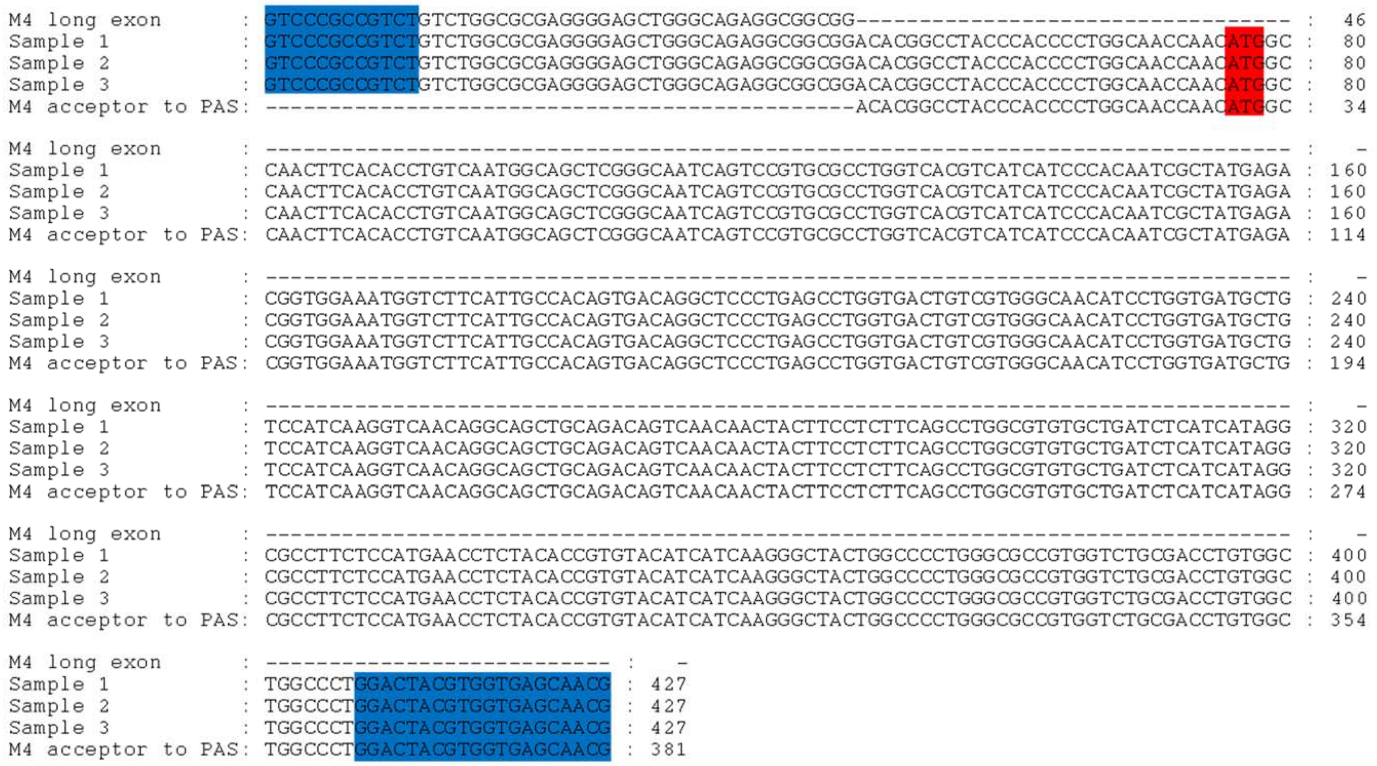

Fig 5. Sequence alignment of the 3 different donor samples used in this study. The sequences are aligned with the upstream M_4L exon sequence (top sequence), has the CG-donor AC-acceptor sequence, and the canonical exon 1 sequence (bottom). The canonical start codon (ATG) is shown in red and blue represents the junction primers used in Fig 4.

https://doi.org/10.1371/journal.pone.0188330.g005

Expression of the M_4S and M_4L

HEK293T cells were transiently transfected with M_4S and M_4L constructs tagged at the N-terminus with myc. The M_4S (theoretical molecular weight = 53kD) and M_4L (theoretical molecular weight = 71kD) were detected in whole cell lysates using a commercially available myc antibody (Fig 6).

Immuno-fluorescence was employed to investigate the cellular distribution of the M_4S and M_4L receptors in a HEK293T cell type stably expressing the constructs (Fig 7). Results indicate that M_4S was mostly localized to the membrane (Fig 7A), conversely the M_4L receptor appeared to localize mostly within the cytoplasm (Fig 7B).

Membranes assessed for saturation binding using [^{3}H]-NMS showed that both M_4S and M_4L were expressed in HEK293T, however B_{max} values were much higher for M_4S when cells were transfected with similar quantities of DNA. Conversely, the affinity (K_d) for [^{3}H]-NMS was nearly identical between M_4S and M_4L 0.13 ± 0.04 and 0.15 ± 0.02nM at 24μg DNA, respectively (Table 1). Overall, expression of both variants was sufficient for pharmacological characterization.

Comparison between the M_4S and M_4L orthosteric site assessed by GTP-γ-[^{35}S] binding

Fig 8A and 8B summarizes the functional concentration response curves for acetylcholine, oxotremorine-M (Oxo-M), McN-A-343 and pilocarpine stimulated GTPγ-[^{35}S] binding in cells transiently expressing M_4S (Fig 8A) and M_4L (Fig 8B).

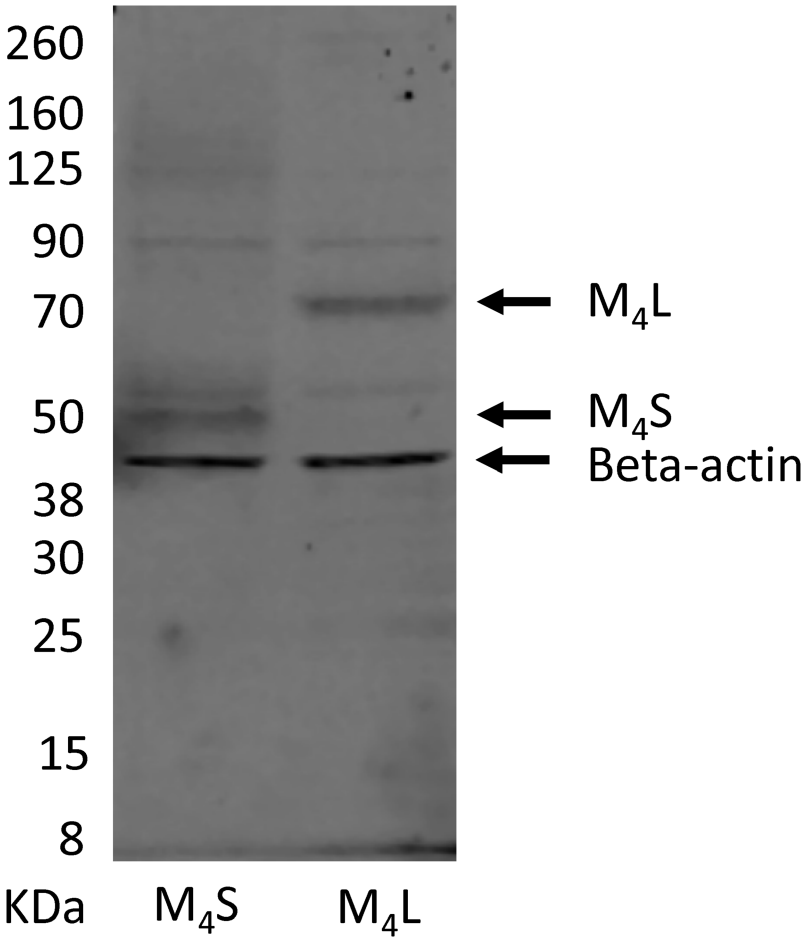

Fig 6. Western blot results for M_4S and M_4L transiently expressed in HEK293T. A representative Western blot on whole cell lysates from transient HEK293T cells expressing the M_4S and M_4L in the presence of an anti-myc antibody and a beta actin loading control monoclonal antibody.

https://doi.org/10.1371/journal.pone.0188330.g006

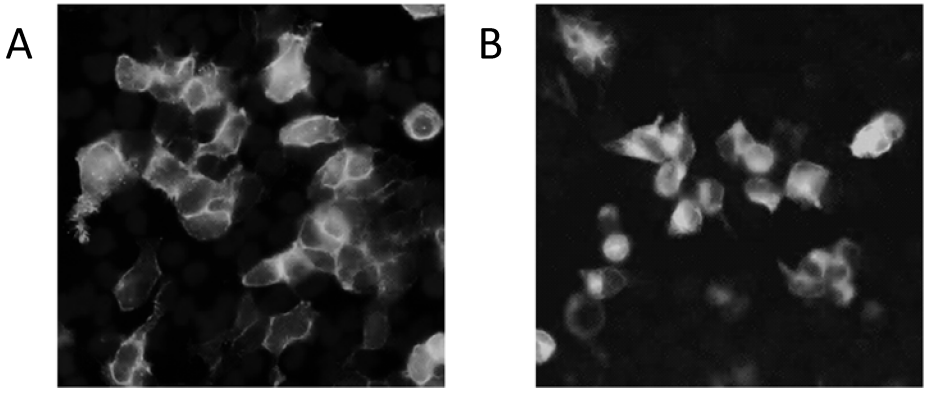

Fig 7. Immunoflorescence showing the distribution of M_4S and M_4L transiently transfected into HEK293T cells. A) Using an anti-myc antibody, image is representative of immunofluorescence of the M_4S receptor transiently expressed in HEK293T cells. B) This image represents immunofluorescence of M_4L transiently expressed in HEK293T cells.

https://doi.org/10.1371/journal.pone.0188330.g007

Table 1. Saturation binding with [^{3}H]-NMS to membranes transiently expressing either M_4S or M_4L in HEK293T.

Receptor—μg DNA	B_{max} (fmol/mg protein)	K_d (nM)
M_4S (48)	3120 ± 290	0.14 ± 0.03
M_4L (48)	152 ± 13.8	0.12 ± 0.03
M_4S (24)	1305 ± 38.5	0.13 ± 0.04
M_4L (24)	745 ± .66.8	0.15 ± 0.02

Data shown are the result of 3 independent experiments performed in duplicate. The numerical values are expressed as the mean ± S.E.M. Using GraphPad unpaired t-test, no significant differences were found between the K_d values for both receptors. However, B_{max} values were statistically significant between M_4S and M_4L at 24 (P = 0.002) and 48 (P = 0.0005) μg DNA.

https://doi.org/10.1371/journal.pone.0188330.t001

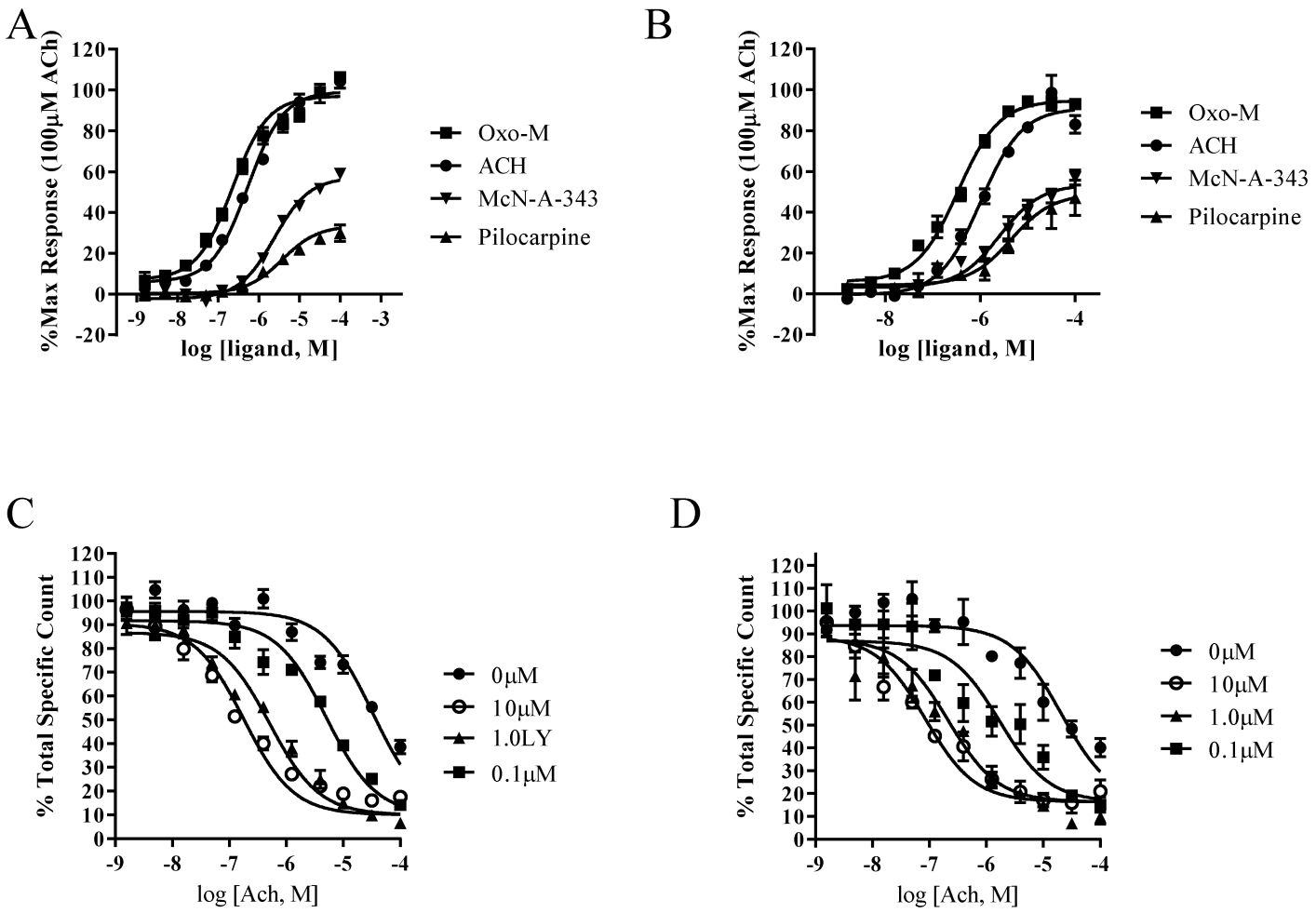

Fig 8. Functional comparison of the orthosteric and allosteric binding sites between the M_4S and M_4L receptors. A) Represents the orthosteric response of the M_4S to known muscarinic agonists: acetylcholine (closed circle), oxotremorine-M (square), pilocarpine (triangle) and McN-A-343 (inverted triangle). B) Summary of the M_4L response for the same 4 muscarinic agonists. C) Graph represents the allosteric response of the M_4S receptor to ACH in the presence of various concentrations of the M_4-PAM, LY2033298. D) Allosteric response of M_4L to ACH in the presence of zero (closed circle), 0,1μM (square), 1.0μM (triangle) or 10μM (open circle) LY2033298. Data shown are the result of 3 independent experiments performed in duplicate.

https://doi.org/10.1371/journal.pone.0188330.g008

Both acetylcholine (circle) and oxo-M (square) displayed full agonist properties at M_4S and M_4L receptors. In addition, the EC_{50} values for acetylcholine and oxo-M were very similar at both receptors. Acetylcholine had an EC_{50} = 619±47.9nM and 714±231nM for the M_4S and M_4L, respectively. Likewise, oxotremorine-M EC_{50} at the M_4S was 310±120nM and 270 ±118nM at the M_4L variant. Both pilocarpine (triangle) and McN-A-343 (inverted triangle) showed partial agonist activity at the M_4L receptor consistent with their known pharmacology at the canonical M_4 receptor. Similar results were found with commercially available membranes containing the canonical M_4S receptor.

Comparison between the M_4S and M_4L allosteric site assessed by [^{3}H]-NMS competitive binding

A series of [^{3}H]-NMS binding experiments were performed to assess whether differences in the allosteric binding sites existed between the M_4S and M_4L receptor variants. The displacement of [^{3}H]-NMS by oxo-M was very similar between the M_4S and M_4L with K_i log values of 5.25±0.10nM and 6.00±0.26nM respectively (Fig 8C and 8D). Competitive binding experiments were then used to assess the function of a common muscarinic allosteric binding site located in the outer extracellular vestibule of muscarinic receptors [19, 20]. Specifically, the potentiation of oxo-M was tested in the presence of varying concentrations of LY2033298, an M4 positive allosteric modulator (M_4-PAM). In the presence of 10μM LY2033298 oxo-M was potentiated 100-fold at both the M_4S and M_4L receptors similar to previous reports [1]. The M_4S receptor had a K_i log value of 7.52 ± 0.06 which was similar to the M_4L which had a K_i log value of 8.05±0.15 at this concentration of an M_4-PAM.

Conclusions

Northern/Western data from the literature support this possibility that the muscarinic receptor family contains splice variants [15, 16]. In fact, a common alternative splice variant was identified in mouse and rat. BY250825.1 and CJ145250.1 are mouse ESTs that show an upstream exon in addition to the exon that contains the currently understood, complete open reading frame. DV213670.1 is a rat EST that covers the comparable two exons. In the open reading frame analysis, there are no in-frame upstream stop codons and the chosen Kozak consensus sequence is not very strong. The splice donor and acceptor sites identified in the mouse and rat genomes for these three ESTs are conserved in the human genome. Comparative genomics reveals that an open reading frame is possible in human, mouse and rat up to a common ATG/methionine that could possibly extend the amino terminus by 155aa. The new Kozak consensus would be GTC CCC ATG a, the new mRNA size (2 exons: new ATG to donor, acceptor to polyA signal) would be 3225 bp, and the new protein size would be 69.7 kDa. Preliminary RT-PCR experiments were performed to detect the human upstream exon and the connectivity of the two exons within a mature mRNA. The expected size for this splice variant was detected, as well as others. Taqman identified that this particular splice variant is also expressed in brain, testes and thymus.

Additional experiments were performed to identify, express and pharmacologically characterize this splice variant at the protein level. Saturation radioligand binding with [^{3}H]-NMS (N-methyl-scopolamine) from HEK293T membranes transiently expressing M_4S and M_4L revealed that new splice variant can be expressed. However, to determine that the M_4L was truly expressed and not just M_4S that had been post-translational modified, the same membranes were subjected to Western blot analysis. Both M_4S and M_4L were tagged at the N-terminus with myc so that they can be identified with a commercially available anti-myc

antibody. Western blot analysis detected in whole cell lysates, bands of 53kD and 71kD, the theoretical molecular weights for M_4S and M4L, respectively. Comparative pharmacological characterization between the M_4L and M_4S receptors revealed that both the orthosteric and allosteric binding sites for both receptors were very similar despite the addition of an N-terminal extension.

It has long been known that alternative splicing was an important post-transcriptional process by which diverse transcripts can be generated from one mRNA precursor and first proposed in 1978 [21]. Alternative splicing has been recognized as a major source of transcriptome and proteome diversity in GPCRs as well [6]. GPCR receptor splice variants could result in a multitude of pharmacological behaviors. Genetic variation in G-protein coupled receptors has been shown to be associated with a wide spectrum of disease phenotypes and predispositions that are of special significance because they are amenable targets for therapeutic agents [22]. The N-terminus has been shown to be the most variable element in GPCRs, ranging from seven to approximately 5900 residues [23]. One important function of the N-terminus is to stabilize the first transmembrane helix to ensure the correct receptor structure. Several alternative splicing of exons encoding the N-terminal domain have been reported and have been shown to display altered ligand affinity as well as differential activation by endogenous ligands. For example, N-terminal splice variants of the type I PACAP receptor has been shown to have both altered binding and cAMP function with the PAC1 ligand. This leads to significant differences in the affinities and selectivity towards PACAP38, PACAP27 and VIP in the tested HEK293 cell model [24].

Here we describe a new splice variant for the muscarinic M_4 receptor. Using a combination of bioinformatics, molecular and cellular biological techniques we have evidence for an N-terminal extension of the M_4 receptor that results in a unique receptor isoform that can be exogenously expressed. In this communication, binding to the orthosteric and allosteric binding pockets for both the M_4S and M_4L receptors were not compromised by altering the N-terminus, but remain very similar to each other. Recent crystallization of the active state of the muscarinic M_2 receptor with both allosteric and orthosteric sites occupied provided detailed information of both binding pockets [19]. Since LY2119620, the M_4 allosteric ligand docked into the active state M_2 crystal also modulates the M_4 receptor, their structural and binding are likely similarity [25, 26]. Therefore, the extension of the N-terminal domain most likely does not provide unique orthosteric or allosteric binding regulation, but that does not rule out that splice variants don't provide an opportunity to redefine the physiology and pharmacology of known muscarinic receptor family.

The most notably different between the M_4S and M_4L was expression when expressed in HEK293T cells. The N-terminal extension isoform appears to have an effect on receptor expression at the membrane. Using immuno-fluorescent, the M_4S receptor appeared to be mostly expressed on the cell membrane (Fig 7A) while M_4L expression appears more cytosolic (Fig 7B). This pattern was irrespective of M_4L expression. This pattern was very reminiscent to the V2a receptor. The V2a receptor did not move to the plasma membrane, but was retained in the ER—Golgi compartment [27]. Our results are very similar to the somatostatin receptor sst5, which has two truncated isoforms named sst5TMD5 and sst5TMD4. In contrast with the predominant plasma membrane localization of full-length sst5, both sst5TMD5 and sst5TMD4 show a preferential intracellular localization [28]. Another splice variants, C1a receptor [29] has also been shown to result in poor receptor expression at the plasma membrane so our findings are not unprecedented. Although the biological implication of the M_4L localization needs to be further explored, mis-localization may not be abnormal since as much 50% of newly synthesized proteins are ER retained [30].

Acknowledgments

The authors acknowledge the technical contributions of Angela Freeman, Kathleen DeBrota, Andrew M. Cooper and Hongling Xiao who contributed to the characterization of the M_4L receptor but who's work was not included in this manuscript

Author Contributions

Conceptualization: Cara L. Ruble, Christian C. Felder.

Data curation: Douglas A. Schober, Carrie H. Croy, Cara L. Ruble, Ran Tao.

Formal analysis: Ran Tao.

Methodology: Douglas A. Schober, Carrie H. Croy, Cara L. Ruble, Ran Tao.

Supervision: Douglas A. Schober, Christian C. Felder.

Writing – original draft: Douglas A. Schober, Carrie H. Croy, Cara L. Ruble, Ran Tao.

Writing – review & editing: Douglas A. Schober, Christian C. Felder.

References

1. Chan WY, McKinzie DL, Bose S, Mitchell SN, Witkin JM, Thompson RC, et al. Allosteric modulation of the muscarinic M4 receptor as an approach to treating schizophrenia. Proc Natl Acad Sci U S A. 2008; 105(31):10978–83. https://doi.org/10.1073/pnas.0800567105 PMID: 18678919
2. Carruthers SP, Gurvich CT, Rossell SL. The muscarinic system, cognition and schizophrenia. Neurosci Biobehav Rev. 2015; 55:393–402. https://doi.org/10.1016/j.neubiorev.2015.05.011 PMID: 26003527
3. Conn PJ, Jones CK, Lindsley CW. Subtype-selective allosteric modulators of muscarinic receptors for the treatment of CNS disorders. Trends Pharmacol Sci. 2009; 30(3):148–55. https://doi.org/10.1016/j.tips.2008.12.002 PMID: 19201489
4. Bymaster FP, McKinzie DL, Felder CC, Wess J. Use of M1–M5 Muscarinic Receptor Knockout Mice as Novel Tools to Delineate the Physiological Roles of the Muscarinic Cholinergic System. Neurochemical Research. 2003; 28(3):437–42. https://doi.org/10.1023/a:1022844517200
5. Gentles AJ, Karlin S. Why are human G-protein-coupled receptors predominantly intronless?: Trends Genet; 1999. 47–9 p. PMID: 10098406
6. Markovic D, Challiss RA. Alternative splicing of G protein-coupled receptors: physiology and pathophysiology. Cell Mol Life Sci. 2009; 66(20):3337–52. https://doi.org/10.1007/s00018-009-0093-4 PMID: 19629391
7. Minneman KP. Splice variants of G protein-coupled receptors. Mol Interv. 2001; 1(2):108–16. PMID: 14993330
8. Sarmiento JM, Añazco CC, Campos DM, Prado GN, Navarro J, González CB. Novel Down-regulatory Mechanism of the Surface Expression of the Vasopressin V2 Receptor by an Alternative Splice Receptor Variant. Journal of Biological Chemistry. 2004; 279(45):47017–23. https://doi.org/10.1074/jbc.M410011200 PMID: 15355989
9. Ji TH, Grossmann M, Ji I. G Protein-coupled Receptors: I. DIVERSITY OF RECEPTOR-LIGAND INTERACTIONS. Journal of Biological Chemistry. 1998; 273(28):17299–302. https://doi.org/10.1074/jbc.273.28.17299 PMID: 9651309
10. Buchli R, Ndoye A, Rodriguez JG, Zia S, Webber RJ, Grando SA. Human skin fibroblasts express m2, m4, and m5 subtypes of muscarinic acetylcholine receptors. J Cell Biochem. 1999; 74(2):264–77. PMID: 10404395
11. Ruble CL, Smith RM, Calley J, Munsie L, Airey DC, Gao Y, et al. Genomic structure and expression of the human serotonin 2A receptor gene (HTR2A) locus: identification of novel HTR2A and antisense (HTR2A-AS1) exons. BMC Genetics. 2016; 17:16. https://doi.org/10.1186/s12863-015-0325-6 PMID: 26738766
12. Carver TJ, Rutherford KM, Berriman M, Rajandream MA, Barrell BG, Parkhill J. ACT: the Artemis Comparison Tool. Bioinformatics. 2005; 21(16):3422–3. https://doi.org/10.1093/bioinformatics/bti553 PMID: 15976072
13. Florea L, Hartzell G, Zhang Z, Rubin GM, Miller W. A computer program for aligning a cDNA sequence with a genomic DNA sequence. Genome Res. 1998; 8(9):967–74. PMID: 9750195

14. Rice P, Longden I, Bleasby A. EMBOSS: the European Molecular Biology Open Software Suite. Trends Genet. 2000; 16(6):276–7. PMID: 10827456

15. Edgar RC. MUSCLE: multiple sequence alignment with high accuracy and high throughput. Nucleic Acids Res. 2004; 32(5):1792–7. https://doi.org/10.1093/nar/gkh340 PMID: 15034147

16. Nicholas KB. GeneDoc: Analysis and visualization of genetic variation. EMBNEW NEWS. 1997; 4:14.

17. Wu TD, Nacu S. Fast and SNP-tolerant detection of complex variants and splicing in short reads. Bioinformatics. 2010; 26(7):873–81. https://doi.org/10.1093/bioinformatics/btq057 PMID: 20147302

18. Sanger F, Coulson AR. A rapid method for determining sequences in DNA by primed synthesis with DNA polymerase. Journal of Molecular Biology. 1975; 94(3):441–8. http://dx.doi.org/10.1016/0022-2836(75)90213-2. PMID: 1100841

19. Kruse AC, Ring AM, Manglik A, Hu J, Hu K, Eitel K, et al. Activation and allosteric modulation of a muscarinic acetylcholine receptor. Nature. 2013; 504(7478):101–6. https://doi.org/10.1038/nature12735 PMID: 24256733

20. Thal D, Sun B, Feng D, Nawaratne V, Leach K, Felder C, et al. Crystal Structures of the M1 and M4 Muscarinic Acetylcholine Receptors and Insights into their Allosteric Modulation. Nature. 2016;In press.

21. Gilbert W. Why genes in pieces? Nature. 1978; 271(5645):501-. PMID: 622185

22. Thompson MD, Burnham WM, Cole DE. The G protein-coupled receptors: pharmacogenetics and disease. Crit Rev Clin Lab Sci. 2005; 42(4):311–92. https://doi.org/10.1080/10408360591001895 PMID: 16281738

23. McMillan DR, Kayes-Wandover KM, Richardson JA, White PC. Very Large G Protein-coupled Receptor-1, the Largest Known Cell Surface Protein, Is Highly Expressed in the Developing Central Nervous System. Journal of Biological Chemistry. 2002; 277(1):785–92. https://doi.org/10.1074/jbc.M108929200 PMID: 11606593

24. Dautzenberg FM, Mevenkamp G, Wille S, Hauger RL. N-terminal splice variants of the type I PACAP receptor: isolation, characterization and ligand binding/selectivity determinants. J Neuroendocrinol. 1999; 11(12):941–9. PMID: 10583729

25. Croy CH, Schober DA, Xiao H, Quets A, Christopoulos A, Felder CC. Characterization of the Novel Positive Allosteric Modulator, LY2119620, at the Muscarinic M2 and M4 Receptors. Molecular Pharmacology. 2014; 86(1):106–15. https://doi.org/10.1124/mol.114.091751 PMID: 24807965

26. Schober DA, Croy CH, Xiao H, Christopoulos A, Felder CC. Development of a Radioligand, [3H] LY2119620, to Probe the Human M2 and M4 Muscarinic Receptor Allosteric Binding Sites. Molecular Pharmacology. 2014; 86(1):116–23. https://doi.org/10.1124/mol.114.091785 PMID: 24807966

27. Gonzalez A, Borquez M, Trigo CA, Brenet M, Sarmiento JM, Figueroa CD, et al. The Splice Variant of the V2 Vasopressin Receptor Adopts Alternative Topologies. Biochemistry. 2011; 50(22):4981–6. https://doi.org/10.1021/bi2001278 PMID: 21534618

28. Durán-Prado M, Gahete MD, Martínez-Fuentes AJ, Luque RIM, Quintero A, Webb SM, et al. Identification and Characterization of Two Novel Truncated but Functional Isoforms of the Somatostatin Receptor Subtype 5 Differentially Present in Pituitary Tumors. The Journal of Clinical Endocrinology & Metabolism. 2009; 94(7):2634–43. https://doi.org/10.1210/jc.2008-2564 PMID: 19401364

29. Seck T, Baron R, Horne WC. The alternatively spliced deltae13 transcript of the rabbit calcitonin receptor dimerizes with the C1a isoform and inhibits its surface expression. J Biol Chem. 2003; 278 (25):23085–93. https://doi.org/10.1074/jbc.M211280200 PMID: 12686555

30. Ellgaard L, Molinari M, Helenius A. Setting the standards: quality control in the secretory pathway. Science. 1999; 286(5446):1882–8. PMID: 10583943